Journal of Biomolecular NMR, **23:** 169–179, 2002.
KLUWER/ESCOM

Order-parameter tensor description of HPr in a medium of oriented bicelles

Franciska van Lune, Linda Manning, Klaas Dijkstra, Herman J.C. Berendsen & Ruud M. Scheek*
Biophysical Chemistry Department, Groningen Institute of Biomolecular Sciences and Biotechnology, University of Groningen, Groningen, The Netherlands

Received 2 January 2002; Accepted 1 May 2002

Key words: alignment, bicelles, HPr, order-parameter tensor, orientation, residual dipolar couplings

Abstract

Residual dipolar couplings between ^{15}N and ^{1}H nuclear spins in HPr were used to determine the protein's orientation in a medium of bicelles, oriented by a magnetic field. In the case of wild-type HPr the protein's non-spherical shape can explain its orientation in this medium. In the case of the F48W mutant it was found that at least one other mechanism contributes to the observed orientation of the protein, to a degree that depends on the concentration of phosphate ions in the medium. We propose that the F48W mutant has a weak affinity towards the bicelle-surfaces that decreases with increasing phosphate concentrations. We used an order-parameter description to analyse this situation and to determine the axis of main order and the sign of the order parameter pertaining to this additional orientation mechanism.

Introduction

Residual dipolar couplings, which can be measured between nuclear spins in a molecule that is prevented from tumbling entirely isotropically in solution, have become an important source of information, complementing nuclear Overhauser effects and J-couplings, for the determination of the three-dimensional structure of proteins in solution (Tjandra and Bax, 1997; Otttiger and Bax, 1998). Alternatively, when a model of the three-dimensional structure of the protein is available, these dipolar coupling measurements can be used to determine the order-parameter tensor that describes the anisotropy of the protein's rotational diffusion in the presence of, for example, magnetically oriented bicelles. Often this observed order-parameter tensor can be explained satisfactorily in terms of the protein's shape, assuming that only an obstruction effect is responsible for the protein's orientational preferences in the presence of oriented bicelles (Zweckstetter and Bax, 2000).

In this paper we present a case where a single mutation (a surface phenylalanine was replaced by a tryptophan) has a significant effect on the protein's order-parameter tensor, which cannot be explained by a change in the overall shape of the mutated protein. Two possible additional orientation mechanisms are examined theoretically and evidence is presented for one of these. This case neatly illustrates the usefulness of the order-parameters tensor description for the analysis of such complications.

Theory

The dipolar interaction energy between two nuclear spins (coordinates: $\mathbf{r}_1$ and $\mathbf{r}_2$; spin angular momenta: $\hbar\mathbf{I}_1$ and $\hbar\mathbf{I}_2$; magnetic moments: μ_1 $(= \gamma_1\hbar\ \mathbf{I}_1)$ and μ_2 $(= \gamma_2\hbar\ \mathbf{I}_2)$) can be written as $E_{dip} = \frac{\mu_0}{4\pi}\frac{1}{r^3}\ \mu_1^T\ \mathbf{D}\ \mu_2$. Here $\mathrm{r} = (|\mathbf{r}_1 - \mathbf{r}_2|)$, the distance between the two spins. We use a matrix notation with vectors represented by a one-column matrix, and ^{T} denoting the

*To whom correspondence should be addressed. E-mail: R.scheek@chem.rug.nl

transpose. **D** is the dipolar interaction tensor:

$$\mathbf{D} = \begin{bmatrix} 3xx-1 & 3xy & 3xz \\ 3xy & 3yy-1 & 3yz \\ 3xz & 3yz & 3zz-1 \end{bmatrix}$$

(x, y, z) are the coordinates of the unit vector connecting the two spins: $(\mathbf{r}_1 - \mathbf{r}_2)/|\mathbf{r}_1 - \mathbf{r}_2|$. With a magnetic field along the z-direction, only the z-components of the magnetic moments (for two spins1/2: $\pm 1/2\ \gamma\hbar$), and hence only the 3,3 element of the interaction tensor, are important for the observable dipolar couplings:

$$E_{dip} = \pm\frac{\mu_0}{4\pi}\frac{1}{4}\gamma_1\gamma_2\hbar^2\left(\frac{3zz-1}{r^3}\right).$$

The observable splitting caused by this dipolar interaction (in Hertz) between heteronuclear spins (for which these dipolar couplings are much smaller than the difference in their Larmor frequencies) becomes (Fischer et al., 1999):

$$D = \frac{\mu_0}{4\pi}\gamma_1\gamma_2\frac{\hbar}{4\pi}\left\langle\frac{3zz-1}{r^3}\right\rangle.$$

Here, triangular brackets indicate time averaging.

Molecular tumbling modulates the interaction between nuclear magnetic moments. The observable dipolar coupling, which is proportional to the rotationally averaged value of the 3,3 element of the dipolar interaction tensor, vanishes if the rotational diffusion is isotropic: the usual situation in solution (Tjandra and Bax, 1997). Under conditions where the rotational diffusion is anisotropic, an order parameter tensor succinctly describes the averaging process (Fowler et al., 2000; Zweckstetter and Bax, 2000). The value of the 3,3 element of the dipolar interaction tensor, averaged over all rotated states identified by a rotation matrix R, can be written as (Samulski and Berendsen, 1972):

$$< (\mathbf{RDR}^T)_{33} >= 2/3Tr(\mathbf{SD}), \quad (1)$$

where the order-parameter tensor **S** is defined as follows:

$$\mathbf{S} = \frac{1}{2}\begin{bmatrix} 3\langle\xi\xi\rangle - 1 & 3\langle\xi\eta\rangle & 3\langle\xi\zeta\rangle \\ 3\langle\xi\eta\rangle & 3\langle\eta\eta\rangle - 1 & 3\langle\eta\zeta\rangle \\ 3\langle\zeta z\rangle & 3\langle\eta\zeta\rangle & 3\langle\zeta\zeta\rangle - 1 \end{bmatrix}.$$

Here, (ξ, η, ζ) are the coordinates in a molecule-fixed coordinate frame of a unit vector, rotating with the molecule and pointing along the z-axis in the unrotated molecular frame. An order parameter tensor is symmetric, with trace zero, so that only five of its elements are independent (see below) (Losonczi et al., 1999; Al-Hashimi et al., 2000). The choice of the molecular coordinate frame is irrelevant: the trace of the matrix product does not change if both tensors **S** and **D** are rotated in the same way.

A given set of dipolar couplings, measured for a large number of spin pairs (i) (D_{exp^i}), can be used to determine the complete order-parameter tensor that minimizes the rms difference between the calculated (D_{calc^i}) and the measured (D_{exp^i}) dipolar couplings. Following Lozonczi et al. (1999) we rearranged the above equations for all spin pairs into a form suitable for their simultaneous solution by singular value decomposition:
For spin pair i:

$$D^i_{\mathrm{calc}} = \frac{\mu_0}{4\pi}\frac{1}{r^3}\gamma_1\gamma_2\frac{\hbar}{4\pi}\langle 2/3Tr(\mathbf{SD}^{\mathrm{i}})\rangle,$$

in which

$$Tr(\mathbf{SD}^{\mathrm{i}}) = \mathbf{d}^{\mathrm{i}}\mathbf{s},$$

defining

$$\mathbf{d}^i = \left(2\mathbf{D}^i_{11} + \mathbf{D}^i_{22}\ 2\mathbf{D}^i_{12}\ 2\mathbf{D}^i_{13}\ 2\mathbf{D}^i_{22} + \mathbf{D}^i_{11}\ 2\mathbf{D}^i_{23}\right)$$

and

$$\mathbf{s} = \begin{pmatrix} \mathbf{S}_{11} \\ \mathbf{S}_{12} \\ \mathbf{S}_{13} \\ \mathbf{S}_{22} \\ \mathbf{S}_{23} \end{pmatrix}.$$

Here we used the fact that both **S** and **D** are traceless and symmetric.

Simultaneous solution (in the least squares sense) of the set of equations:

$$\frac{\mu_0}{4\pi}\frac{1}{r^3}\gamma_1\gamma_2\frac{\hbar}{4\pi}2/3\mathbf{d}^i\mathbf{s} = D^i_{\mathrm{exp}} \quad (2)$$

yields the five elements of **s** (and **S)** that minimize the rms differences between measured and calculated dipolar couplings. This experimentally determined $\mathbf{S}_{\mathrm{exp}}$ can be interpreted in terms of one (or more) orientation mechanisms. We used the algebra program Mathematica™ (Wolfram Research Inc.) to perform these calculations.

*Prediction of the order-parameter tensor **S** based on molecular shape*

In an environment of magnetically aligned bicelles, a non-spherical molecule will be aligned preferentially with its longest axis parallel to the bicelle surfaces. This effect can be understood as an obstruction effect on the orientation. In the absence of other orientation

mechanisms the order-parameter tensor that describes this situation can be calculated if the shape of the molecule is known. To calculate the order-parameter tensor for a protein with a given three-dimensional structure, we use an isotropically distributed ensemble of N (typically 1000) rotated protein molecules and calculate for each rotated state the longest extension of the rotated molecule along the z-axis. The matrix elements that need to be averaged over all rotated states to yield the order-parameter tensor, are given a weight proportional to the longest z-extension ($\Delta z_{\max}$) of the molecule in the corresponding rotated state. For example, the 1,1 element of the order-parameter tensor (apart from a scaling factor: see below) becomes:

$$\mathbf{S}_{11} = \langle 3xx - 1 \rangle$$

$$= \left[\sum_{i=1}^{N} (3x_i x_i - 1).(\Delta z_{\max})_i \right] \Big/ \sum_{i=1}^{N} (\Delta z_{\max})_i ,$$

where the averaging is over the N rotated states (i). This procedure yields a tensor, which can be written as a rotated diagonal tensor as follows:

$$\mathbf{S} = \mathbf{R}\mathbf{S}^{\mathrm{d}}\mathbf{R}^{\mathrm{T}} = \mathbf{R} f \begin{bmatrix} -\frac{1}{2}(1-\eta) & 0 & 0 \\ 0 & -\frac{1}{2}(1+\eta) & 0 \\ 0 & 0 & 1 \end{bmatrix} \mathbf{R}^{\mathrm{T}}, \quad (3)$$

with $|\mathbf{S}^{\mathrm{d}}_{33}| > |\mathbf{S}^{\mathrm{d}}_{22}| > |\mathbf{S}^{\mathrm{d}}_{11}|$. This defines f ($= \mathbf{S}^{\mathrm{d}}_{33}$) as an overall order parameter, and η ($= (\mathbf{S}^{\mathrm{d}}_{11} - \mathbf{S}^{\mathrm{d}}_{22})/\mathbf{S}^{\mathrm{d}}_{33}$) as an asymmetry parameter ($0 \leq \eta \leq 1$), that is determined by the deviation of the molecular shape from axial symmetry around the principal order axis.

The overall order parameter is not only determined by the molecular dimensions, but also by the average distance between the bicelle surfaces, and hence by the bicelle concentration. In this work we do not attempt to calculate the value of f for a given set of sample conditions, but we choose to treat it as an empirical scaling factor. In this case, the asymmetry parameter η as well as the three angles that determine the orientation of the order parameter tensor in the unrotated molecular coordinate system, are determined by the molecule's shape alone.

Given model coordinates of, e.g., a protein, $\mathbf{S}_{\mathrm{shape}}$ (apart from a factor) and $\mathbf{D}^i$ can be calculated in this coordinate frame for each pair (i) of interacting spins. Equation (1) then yields the dipolar coupling (again apart from a factor) to be expected for this spin pair, under the assumption that the molecule's shape alone determines its orientation in the bicelle medium. The overall order parameter (the missing factor) can be determined by minimizing the rms difference between calculated and measured dipolar couplings.

In cases where $\mathbf{S}_{\mathrm{exp}}$ and $\mathbf{S}_{\mathrm{shape}}$ are significantly different the difference between these two $\mathbf{S}$ tensors may be interpreted in terms of one or more additional orientation mechanisms. Assuming one additional orientation mechanism that would yield an axially symmetric order-parameter tensor, and assuming that the three-dimensional structure of the molecule is not affected by any of the orientation mechanisms, this system can be solved and the preferred orientation under this additional mechanism determined:

$$\mathbf{S}_{\mathrm{exp}} = f_{\mathrm{shape}}\mathbf{S}^{\mathbf{o}}_{\mathrm{shape}} + f_2\mathbf{S}^{\mathbf{o}}_2$$

In cases where $\mathbf{S}_{\mathrm{exp}}$ changes with sample conditions (e.g., the phosphate concentration: see below), a similar analysis may provide information about the part of the orientation mechanism that depends on those sample conditions. Two additional orientation mechanisms are considered in this work: Intermolecular interactions between the protein and the bicelles, and aggregation of protein molecules to form dimers. In all these cases the tensor describing the overall order is simply the weighted sum of the order-parameter tensors pertaining to each ordering mechanism.

Protein-bicelle interactions

Specific interaction between a protein interface and the flat surfaces of the bicelles defines an axis in the protein that, like the axis normal to the bicelle-surfaces, tends to avoid the magnetic field direction. This situation is described by an axially symmetric order-parameter tensor with a negative order parameter along this axis. In a rigid model the order parameter equals the fraction of bound protein molecules. If the interaction is weak and if the exchange between bound and free forms of the protein is fast its effect on chemical shifts and linewidths of protein resonances may be insignificantly small, but the measured residual dipolar couplings may be significantly affected and used to characterise the protein-bicelle interactions. The underlying assumption in such an analysis is that the protein's conformation does not change significantly when bound to the bicelle surface. This is reasonable for most parts of the protein, but structural changes in the binding interface can be expected that will affect the dipolar couplings between spins in this region.

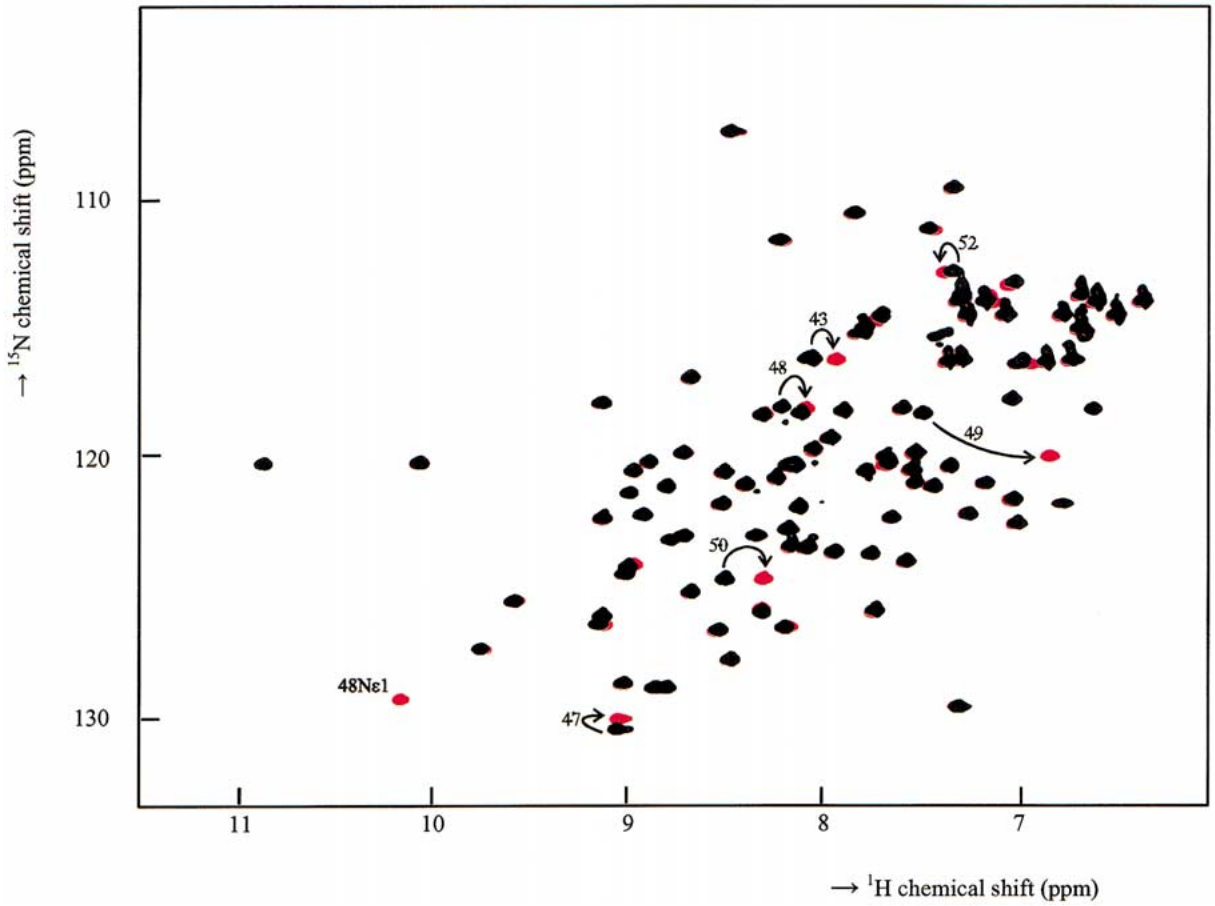

Figure 1. The differences between the HSQC spectra of HPr-WT (black) and HPr-F48W (red). Both spectra were recorded at 20 °C on samples containing 1.5 mM [^{13}C, ^{15}N] HPr-WT and 1.9 mM [^{15}N] HPr-F48W resp. dissolved in 100 mM KP_i pH 6.5 and 7.0 resp. The numbers represent the residue numbers that shift on mutation of Phe48.

Protein dimerisation

Because the overall shape of a protein will be affected by dimerisation, its orientation in a medium of magnetically ordered bicelles will be affected by dimerisation as well. In this situation a new axis of positive order is created, which coincides with the long axis of the dimer. The overall order-parameter tensor is the sum of the tensors describing the orientation of the protein in the monomer and dimer states, each weighted by the fraction of the protein molecules in each of those states. Similar to the previous case structural changes in the dimerisation interface can be expected that will affect the dipolar couplings between spins in this interaction region.

A simple case

Assume a protein has an axially-symmetric shape and is oriented with its long axis along the z-axis of the coordinate system. Such a shape will yield an orientation described by the following order-parameter tensor:

$$\mathbf{S}_{\text{shape}} = f_1 \mathbf{S}^{\mathbf{o}}_{\text{shape}}; \mathbf{S}^{\mathbf{o}}_{\text{shape}} = \begin{bmatrix} -\frac{1}{2} & 0 & 0 \\ 0 & -\frac{1}{2} & 0 \\ 0 & 0 & 1 \end{bmatrix},$$

with $f_1 > 0$ (positive order). Note that we use the superscript $^{\circ}$ to denote a (possibly rotated) normalised tensor (overall order parameter $= +1$).

When this protein interacts with the bicelle surfaces along its y-axis (that is, with a binding interface perpendicular to the y-axis), this will introduce an

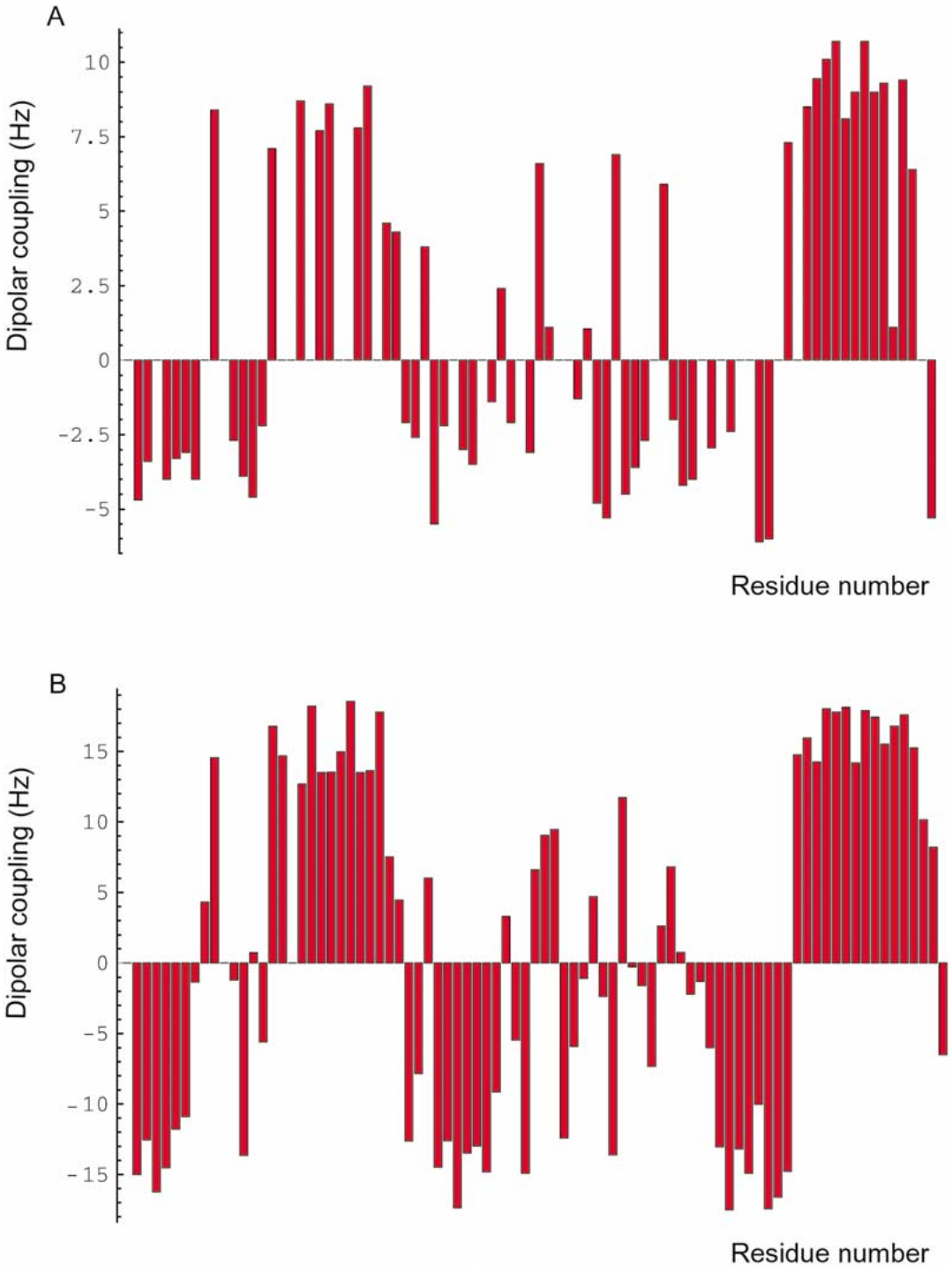

Figure 2. Experimentally determined dipolar couplings of HPr-WT (A) and HPr-F48W (B). Spectra were recorded at 35 °C (anisotropic) and 20 °C (isotropic) on samples containing 1.2 mM [^{15}N] HPr-WT and 1.4 mM [^{15}N] HPr-F48W (10% D_2O, 100 mM KP_i pH 7.0 and 4 % w/v bicelles with a molar ratio DMPC:DHPC of 2.9:1).

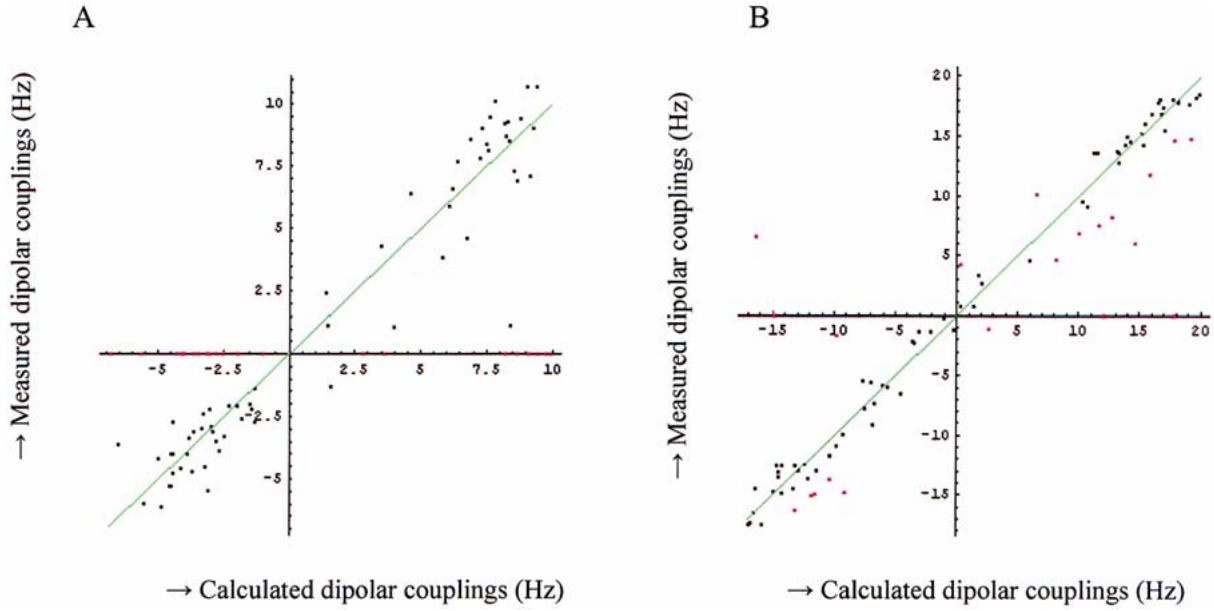

Figure 3. Dipolar couplings determined experimentally for (A) HPr-WT (correlationcoefficient is 0.962) and (B) HPr-F48W (correlationcoefficient is 0.996) compared to dipolar couplings calculated from the X-ray structure of HPr (PDB code: 1opd). Black dots represent dipolar couplings used for calculation of the order-parameter tensor (see text). The red dots represent the remaining dipolar couplings. Red dots on the horizontal axis reflect dipolar couplings that could not be measured.

additional order, described by

$$\mathbf{S}_2 = f_2\mathbf{S}_2^{\mathbf{o}};\ \mathbf{S}_2^{\mathbf{o}} = \begin{bmatrix} -\frac{1}{2} & 0 & 0 \\ 0 & 1 & 0 \\ 0 & 0 & -\frac{1}{2} \end{bmatrix}$$

with $f_2 < 0$ (negative order); in this model $|f_2|$ equals the fraction of the protein that is bound to the bicelles. Together these two orientation mechanisms will yield an overall order that is described by the sum of their respective order-parameter tensors:

$$\mathbf{S} = \mathbf{S}_{\text{shape}} + \mathbf{S}_2 = f_1 \begin{bmatrix} -1/2(1+r) & 0 & 0 \\ 0 & -1/2(1-2r) & 0 \\ 0 & 0 & 1-r/2 \end{bmatrix}$$

defining r as the (in this case negative) ratio f_2/f_1. Note that this may introduce a significant asymmetry ($\eta = -3r/(2-r)$), when defined as in Equation 3 in the overall order parameter tensor. Furthermore, when f_2 dominates f_1 ($r < -1$) the axis of main order will change from the z-axis to the y-axis.

Materials and methods

1,2 dimyristoyl-*sn*-glycero-3-phosphocholine (DMPC), 1,2-dicaproyl-*sn*-glycero-3-phosphocholine (DHPC) and 1,2-dimyristoyl-*sn*-glycero-3-phosphoethanolamine-*N*-[poly-(ethylene glycol 2000] (PEG2000-PE) were purchased as dry powders from Avanti Polar Lipids. $(^{15}NH_4)_2SO_4$ (99.5% [^{15}N]-enriched) was obtained from Campro Scientific. All other materials were from commercial sources.

Expression vectors and bacterial strains

For the production of HPr-WT the plasmid pAB65 described by Lee et al., (1982), which contains the ptsH-gene, was transformed to *E. coli* HB2154 by using standard procedures as described by Sambrook et al., (1989).

The mutant HPr-F48W was constructed by a two-step PCR procedure described by Landt et al. (1990). The plasmid pRB4#1 was used for overexpression of the mutant F48W and was transformed to the *E. coli* strain ZSC112ΔHIC, which is a *glk ptsG manZ ptsH* Δ*ptsI crr* mutant (Mao et al., 1995).

Production of ^{15}N-enriched HPr-WT

E. coli HB2154 cells containing the plasmid pAB65 were pre-grown at 37 °C on Luria–Bertani medium containing 100 μg/ml ampicillin to the exponential phase (A_{600} = 0.6) and transferred to 4 l of M9

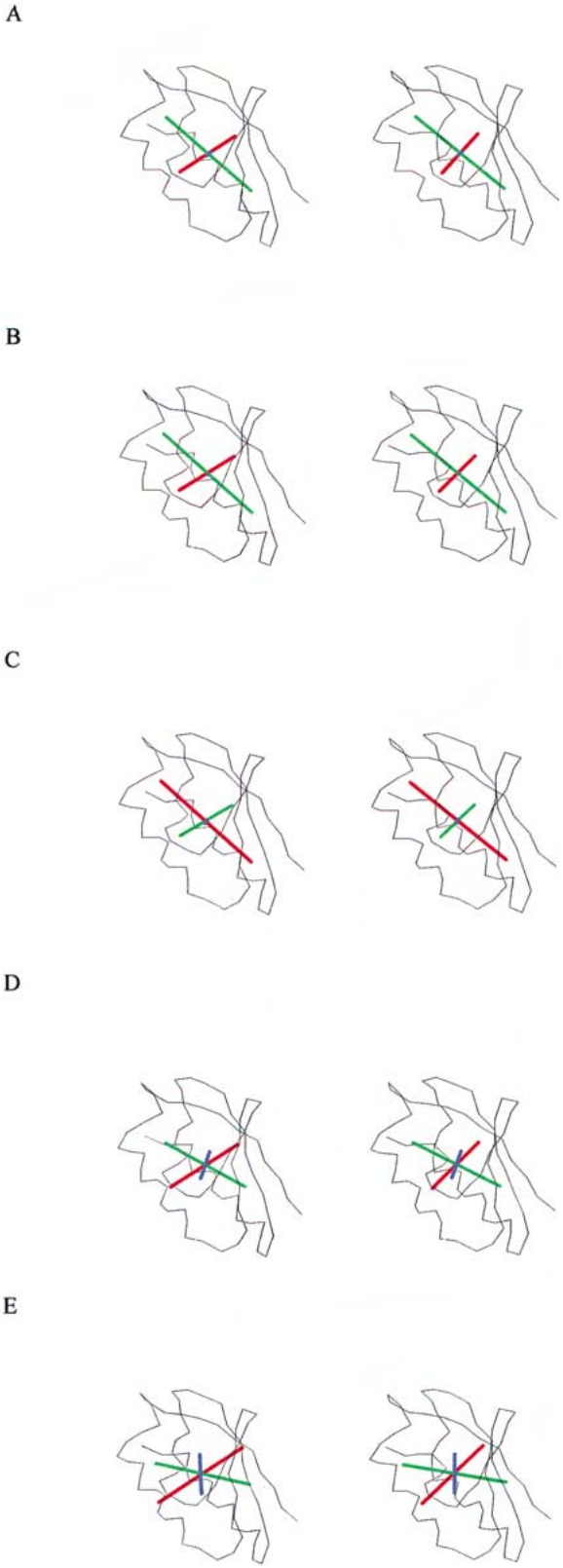

mineral medium containing 5 g/l glucose and 1 g/l $(^{15}NH_4)SO_4$ (Sambrook et al., 1989). Cells were allowed to grow for 24 h at 37 °C and harvested by centrifugation (8000 rpm, 10 min).

Production of ^{15}N-enriched HPr-F48W

^{15}N-labeled HPr-F48W was produced in the same way as wild-type HPr. *E. coli* ZSC112ΔHIC cells containing the plasmid pRB4#1 were pre-grown at 37 °C on Luria-Bertani medium containing 100 μg/ml ampicillin, and transferred to 5 l of M9 mineral medium. Cells were allowed to grow for 18 hours at 37 °C and harvested by centrifugation (8000 rpm, 10 min).

Purification of ^{15}N-enriched HPr-WT and HPr-F48W

The purification was done as described by Van Dijk et al. (1990). 37.5 mg [^{15}N]-enriched HPr-WT and 73.8 mg [^{15}N]-enriched HPr-F48W was obtained after purification.

HPr activity assay

The HPr-activity was followed by determination of [^{14}C]-mannitol phosphorylation as described by Robillard and Blaauw (1987).

Bicelle preparation

The bicelle samples contained 4% w/v DMPC and DHPC ([DMPC]:[DHPC]=2.9), in 100 mM phosphate buffer, pH 7.0 (10% ^2H_2O). Protein was added to the samples after sonication (10 s) of the bicelle

Figure 4. Best-fit order parameter-tensors for HPr-F48W at 45 (A), 80 (B), 100 (C), 500 (D) and 688 (E) mM KP_i . Data were recorded at 35 °C (anisotropic) and 20 °C (isotropic) on samples containing 1.4 mM [^{15}N] HPr-F48W (10% D_2O, pH 7.0 and 4% w/v bicelles with a molar ratio DHPC:DMPC of 2.9:1). Best-fit order-parameter tensors were calculated as described in the text. Shown in red, green and blue are the three eigenvectors, each multiplied by its corresponding eigenvalue, and drawn in both positive and negative directions from the center of mass of the protein. The protein is displayed as a Cα-tracing of the X-ray model used (1opd). (A) $S_{11} = 5.26 \times 10^{-4}$; $S_{12} = 4.14 \times 10^{-5}$; $S_{13} = -3.85 \times 10^{-4}$; $S_{22} = -8.39 \times 10^{-4}$; $S_{23} = -1.71 \times 10^{-4}$. (B) $S_{11} = 5.43 \times 10^{-4}$; $S_{12} = 5.20 \times 10^{-5}$; $S_{13} = -4.28 \times 10^{-4}$; $S_{22} = -8.72 \times 10^{-4}$; $S_{23} = -1.48 \times 10^{-4}$. (C) $S_{11} = 5.43 \times 10^{-4}$; $S_{12} = 5 \times 10^{-5}$; $S_{13} = -4.50 \times 10^{-4}$; $S_{22} = -8.57 \times 10^{-4}$; $S_{23} = -1.24 \times 10^{-4}$. (D) $S_{11} = 6.34 \times 10^{-4}$; $S_{12} = -9.36 \times 10^{-5}$; $S_{13} = -1.98 \times 10^{-4}$; $S_{22} = -9.02 \times 10^{-4}$; $S_{23} = -2.20 \times 10^{-4}$. (E) $S_{11} = 8.06 \times 10^{-4}$; $S_{12} = -2.19 \times 10^{-4}$; $S_{13} = -8.87 \times 10^{-5}$; $S_{22} = -1.03 \times 10^{-3}$; $S_{23} = -3.11 \times 10^{-4}$.

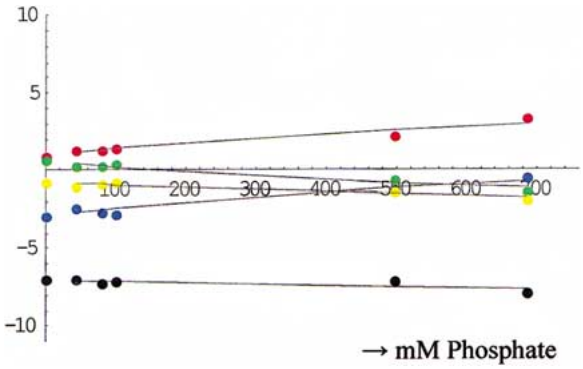

Figure 5. Experimentally observed orientation tensors as a function of the phosphate concentration; red=S_{11}; green=S_{12}; yellow=S_{23}; blue=S_{13}; black=S_{22}. The values on the y-axes need to be divided by $(\mu_0/4\pi)(1/r^3)\gamma_1\gamma_2(\hbar/4\pi)$ (6083 Hz) to get the actual order-parameter tensor elements.

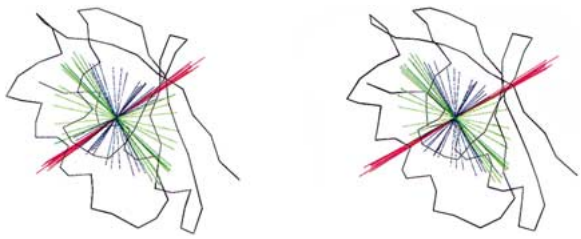

Figure 6. Phosphate-concentration dependent part of the order-parameter tensor of F48W, calculated from the tensors displayed in Figure 4. To the tensors shown in Figure 4 10% noise was added before the phosphate dependent part was extracted, as described in the text. The variations show that the axis of main order of this axially symmetric tensor is not very sensitive to these uncertainties.

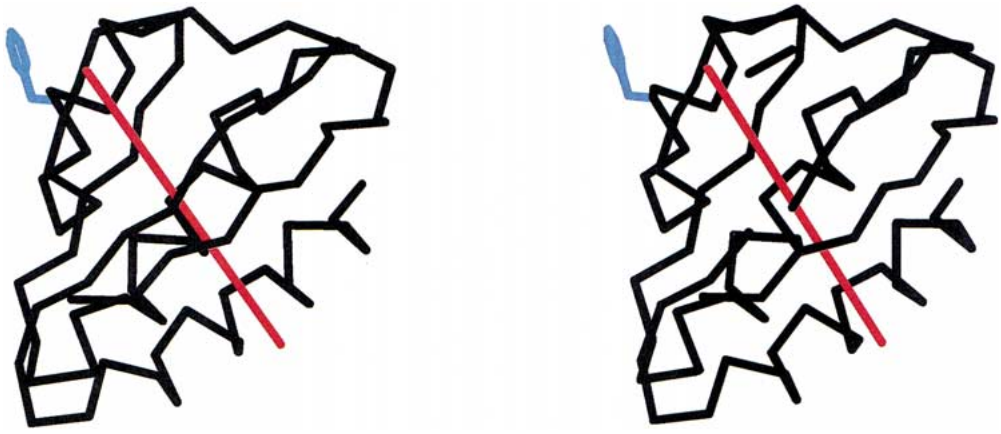

Figure 7 Backbone representation of the X-ray model of HPr-WT. The phenylalanine at position 48 (mutated to a tryptophan in the F48W mutant) is colored blue. The red line is the axis along which HPr-F48W appears to interact with the bicelle surfaces (the average of the red lines in Figure 6).

samples. This procedure resulted in samples with reproducible orientation properties.

Bicelle samples to which a small amount of 1,2-dimyristoyl-*sn*-glycero-3-phosphoethanolamine-*M*-[poly(ethyleneglycol)2000] (PEG2000-PE) was added were prepared to study the influence of the phosphate concentration on the order parameter tensor. The same procedure as described above was used for these samples, except that 1% molar PEG2000-PE was added to the samples before adjusting the pH to pH = 7 with K_2HPO_4 (King et al., 2000). Bicelle samples containing PEG2000-PE were made with 45, 80, 100, 500 and 688 mM KP_i.

It is important to note that all anisotropic data are obtained by inserting a cold sample (4 °C) into a pre-heated probe (35 °C). Isotropic data are recorded at 20 °C.

NMR samples and measurements

All experiments were carried out on a 600 MHz Varian Inova spectrometer. A J_{NH}-modulated HSQC experiment was used to measure the ^1H-^{15}N couplings (Tjandra et al., 1996). Samples were allowed to equilibrate at the desired temperature for at least 15 min prior to acquisition of the NMR data.

Data processing and analysis

All data were processed on a Silicon Graphics O2 workstation, using the program SNARF, written by Frans van Hoesel, Groningen. Mathematica™ was used to calculate dipolar couplings from known structures of HPr and to calculate the order-parameter tensor that minimizes the squared differences between calculated and measured dipolar couplings.

Results and discussion

Figure 1 shows the ^{15}N-^{1}H J-correlation spectra of wild-type HPr and the F48W HPr mutant, measured in 100 mM KP_i buffers, in the presence of DMPC/DHPC bicelles. Clearly, the majority of resonances has remained unaltered and only a few resonances from nuclei near the mutation site have shifted. We conclude that the overall HPr structure has not changed significantly by the mutation. Attempts to record such spectra in the presence of bicelles for HPr-WT and HPr-F48W in 10 mM KP_i, pH 7.0, were only successful for the wild-type HPr: severe line broadening caused most of the resonances of HPr-F48W to disappear. Addition of KCl (up to 180 mM) did not improve this situation, and only after increasing the phosphate concentration to 100 mM or higher could good quality HSQC spectra be recorded.

Figures 2A and 2B show the measured dipolar couplings between the backbone ^{15}N and $^{1}H_N$ nuclei of both forms of HPr in 100 mM KP_i, plotted versus the residue number. We can conclude that the dipolar couplings of the wild-type HPr (Figure 2A) are distributed differently around zero than those of the mutant (Figure 2B). In Figure 2A the dipolar couplings are distributed asymmetrically around zero, reflecting the function $3\ \cos^2\theta - 1$ (rhombicity close to zero) (Tjandra and Bax, 1997). In contrast to the wild-type the mutant has a symmetrical distribution around zero. In the latter case the dipolar couplings reflect the function $3\cos^2\theta - 1 - \sin^2\theta\cos(2\phi)$ (high degree of rhombicity).

We used the datasets presented in Figure 2, together with an X-ray model of HPr's solution conformation (PDB code: 1opd) to find the order-parameter tensor **S** that reproduces best a subset of the measured dipolar couplings. The choice of this subset was made as follows. Dipolar couplings were considered outliers and excluded from the dataset if they differ more than 2 times the standard deviation from the calculated value. With this reduced dataset a new order-parameter tensor was calculated and the procedure was repeated until not more than one outlier remained. This conservative approach was chosen mainly because of uncertainties about the model coordinates and resulted in datasets which consist of 65 dipolar couplings on average, with most of the outliers in the undefined regions or close to the mutation site.

Figures 3A and 3B show a scatter plot of the measured versus the best-fit calculated dipolar couplings for both proteins. The best-fit order-parameter tensors that were calculated from these two datasets are significantly different (supplementary material), suggesting that these very similar proteins are oriented by different mechanisms.

We then switched to a bicelle system to which a small amount (1% molar to DMPC) of polyethyleneglycol-ated DMPC was added (King et al., 2000). As reported by others, these bicelles are more stable and in our case this system allowed us to measure spectra of the F48W mutant in the presence of phosphate concentrations ranging from 45 mM to 688 mM KP_i. The best-fit order parameter tensors found under these conditions are depicted in Figure 4. Clearly, at the lowest phosphate concentration the observed order is different from that observed at the highest concentrations. Changes in the protein cannot be responsible for this effect, because such changes would certainly give rise to significant differences in the HSQC spectra, which we did not observe. Changes in the bicelles themselves are unlikely to explain the observed effects, because the effects were not observed for wild-type HPr (up to 100 mM KP_i). To analyse the observed phosphate effect on the mutant's orientation we write the observed overall orientation tensor as the sum of two tensors as follows:

$$\mathbf{S}_{\text{exp}} = (1 - |f_2|)\mathbf{S}_1 + f_2\mathbf{S}_2^{\mathbf{o}}$$

and interpret $|f_2|$ as the fraction of protein bound to the bicelles, as explained in the theory section:

$$|f_2| = -f_2 = (E_b + EP_b)/(E_b + E_f + EP_b + EP_f),$$

where EP and E stand for the concentrations of the protein with and without phosphate bound to it, respectively, and the subscripts b and f for the protein bound to the bicelles or free in solution, respectively. So we assume that in the absence of phosphate a small fraction K of the protein is bound to the bicelles ($K = E_b/E_f$; $K << 1$), whereas an even smaller fraction $K \cdot \rho$ ($K \cdot \rho = EP_b/EP_f$) is bound at a saturating phosphate concentration ($\rho < 1$). Hence we can

write:

$$\mathbf{S}_{\text{exp}} = \mathbf{S}_1 - \mathbf{S}_2^{\text{o}} \cdot (E_b + EP_b)/(E_f + EP_f).$$

With a dissociation constant k_d describing the affinity of the protein for phosphate ions, this equation can be rearranged as follows:

$$\mathbf{S}_{\text{exp}} = \mathbf{S}_1 - K \cdot \mathbf{S}_2^{\text{o}} \cdot (k_d + \rho \cdot [P_i])/(k_d + [P_i]), \quad (4)$$

where $[P_i]$ stands for the concentration of phosphate ions.

Equation 4 describes a transition of $\mathbf{S}_{\text{exp}}$ from a value of $\mathbf{S}_1 - \mathbf{S}_2^{\text{o}} \cdot K$ in the absence of phosphate to a value of $\mathbf{S}_1 - \mathbf{S}_2^{o} \cdot K \cdot \rho$ at saturating phosphate concentrations.

A least-squares fit of the experimentally observed order-parameter tensors to Equation 4 yields the result shown in Figure 5. Not surprisingly, the normalized order-parameter tensor $\mathbf{S}_2^{\text{o}}$, which describes the protein interaction when bound to the bicelle, is virtually axially symmetric. The orientation of its main axis varies only marginally with reasonable choices of ρ (<1, so phosphate is assumed to decrease the affinity of the protein for the bicelle-surfaces) and k_d (consistent with the observation that the phosphate effect is not saturated at the highest concentrations used).

To estimate the uncertainties in the order-parameter tensors we added random noise (up to $\pm$ 2 Hz) to the measured dipolar couplings and observed the resulting variations in the best-fit order-parameter tensors themselves. This caused variations in the order-parameter tensors that were comparable to the variations observed when different NMR models of HPr (PDB code: 1hdn) were used ($\pm$ 10%). Addition of 10% random noise to the elements of the experimentally observed order-parameter tensors resulted in variations in the tensors $\mathbf{S}_1$ and $\mathbf{S}_2$, as shown for $\mathbf{S}_2$ in Figure 6. From these calculations we conclude that the axis along which HPr-F48W appears to interact with the bicelle surface can be determined with quite reasonable accuracy. If our interpretation is correct, the tryptophan at position 48 in the F48W mutant, which is positioned at the outside of the protein (Figure 7), must be responsible for the interaction with the bicelles, since this interaction does not occur with the wild-type HPr. The affinity of tryptophans for the membrane-water interface (Ridder et al., 2000) may be relevant in this view.

Conclusion

When a model of the three-dimensional structure of a protein is available, dipolar coupling measurements can be used to determine the orientation of the protein in the presence of an oriented liquid crystalline medium like bicelles. If the observed orientation can not be explained by the shape of the protein, additional mechanisms like dimerisation or intermolecular interactions may play a role.

In our case we examined the differences between the orientation of HPr-WT and HPr-F48W in KP_i-buffers of varying concentrations. We discovered that the orientation of the mutant protein F48W depends on the phosphate concentration in contrast to the orientation of the wildtype protein, which is independent of the phosphate concentration. The difference between the orientation of the mutant and the wildtype proteins can be explained by interactions between the bicelles and the protein HPr-F48W. If this interpretation is correct, the data can be analysed to yield the axis in the protein along which this interaction takes place.

The method used in this study may be useful in studies of weak binding interactions between membrane-bound proteins or protein fragments, embedded in the bicelles, and soluble proteins. The effect of the membrane-bound protein or protein fragment on the orientation of the soluble protein, may yield valuable information about the binding interface.

Acknowledgements

We thank Gea Schuurman-Wolters and Ria Duurkens for assistance with the protein production and purification. Frans van Hoesel is gratefully acknowledged for writing the program SNARF, which was used for all data processing and analysis of NMR spectra.

Supplementary material

The order-parameter tensors calculated from the dipolar couplings of wild-type HPr and HPr-F48W in ordinary bicelles at 100 mM KP_I, as well as tables containing the experimentally determined dipolar couplings of HPr-F48W at 45, 80, 100, 500 and 688 mM KP_i in polyethylene-glycol-ated bicelles are available from the corresponding author.

References

Al Hashimi, H.M., Valafar, H., Terrell, M., Zartler, E.R., Eidsness, M.K. and Prestegard, J.H. (2000) *J. Magn. Reson.*, **143**, 402–406.

Fischer, M.W., Losonczi, J.A., Weaver, J.L. and Prestegard, J.H. (1999) *Biochemistry*, **38**, 9013–9022.

Fowler, C.A., Tian, F., Al Hashimi, H.M. and Prestegard, J.H. (2000) *J. Mol. Biol.*, **304**, 447–460.

King, V., Parker, M. and Howard, K.P. (2000) *J. Magn Reson.*, **142**, 177–182.

Landt, O., Grunert, H.P. and Hahn, U. (1990) *Gene*, **96**, 125–128.

Lee, L.G., Britton, P., Parra, F., Boronat, A. and Kornberg, H. (1982) *FEBS Lett.*, **149**, 288–292.

Losonczi, J.A., Andrec, M., Fischer, M.W. and Prestegard, J.H. (1999) *J. Magn Reson.*, **138**, 334–342.

Mao, Q., Schmunk, T., Gerber, B. and Erni, B. (1995) *J. Biol. Chem.*, **270**, 18295–18300.

Ottiger, M. and Bax, A. (1998) *J. Biomol. NMR*, **12**, 361–372.

Ridder, A.N.J.A., Morein, S., Stam, J.G., Kuhn, A., de Kruijff, B. and Killian, J.A. (2000) *Biochemistry*, **39**, 6521–6528.

Robillard, G.T. and Blaauw, M. (1987) *Biochemistry*, **26**, 5796–5803.

Sambrook, C.R., Fritsch, E.F. and Maniatis, T. (1989) *Molecular Cloning*, Cold Spring Harbor Laboratory Press, Cold Spring Harbor, NY.

Tjandra, N. and Bax, A. (1997) *Science*, **278**, 1111–1114.

van Dijk, A.A., de Lange, L.C., Bachovchin, W.W. and Robillard, G.T. (1990) *Biochemistry*, **29**, 8164–8171.

Zweckstetter, M. and Bax, A. (2000) *J. Am. Chem. Soc.*, **120**, 3791–3792.